Check for updates

*CORRESPONDENCE
Zhongyu Qi,
✉ qizhongyu@nbufe.edu.cn
Ce Sun,
✉ sunce@nefu.edu.cn

†These authors have contributed equally
to this work

Cross-linked structures reinforced the bamboo fiber/poly(lactic acid) composites with high heat resistance and their environmental impact through the life cycle assessment analysis

Hui Chen[1†], Pengrui Chen[2†], Zhongyu Qi[3]* and Ce Sun[2]*

[1]School of Economics and Management, Northeast Forest University, Harbin, China, [2]Key Laboratory of Bio-Based Material Science and Technology (Northeast Forestry University), Ministry of Education, Harbin, China, [3]Collage of Digital Technology and Engineering, Ningbo University of Finance and Economics, Ningbo, China

In order to prepare low-cost and heat-resistant poly(lactic acid) (PLA) composites, in this study, bamboo fiber (BF) was added to stereo-complex crystal PLA (SC-PLA) to prepare heat-resistant composites. Poly[(phenyl isocyanate)-co-formaldehyde] [a polyaryl polymethylene isocyanate (PAPI)] was used to form cross-linked structures between SC-PLA and BF, and the effects of PAPI-cross-linked structures on the crystallization properties, mechanical properties, and heat resistance of BF/SC-PLA composites with different BF contents were systematically investigated. When 15% BF was added, the mechanical properties of the composite were significantly improved. The tensile strength increased by 85.5% compared to the unmodified composite, reaching 34.7 MPa, which was even higher than that of the SC-PLA composite (33.1 MPa). In addition, in order to explore the impact of the PAPI-modified BF/SC-PLA composite on the environment and carbon emissions, a life cycle assessment (LCA) of the composites was conducted. The addition of BF effectively reduced the impact of the composite on the environment. Notably, the emissions of CO_2 decreased by approximately 11.7%, and the freshwater, marine, and land ecotoxicity were also significantly reduced. This work provided a reference for the preparation of low-cost and heat-resistant PLA composites for heat-resistant food packaging and disposable tableware and expanded the application of PLA products in the field of heat-resistant materials.

KEYWORDS

bamboo fiber, poly(lactic acid), stereo-complex crystals, life cycle assessment, poly-D(lactic acid)

1 Introduction

In order to address the serious environmental pollution caused by disposable petroleum-based plastics and the large amount of carbon emissions generated during

GRAPHICAL ABSTRACT
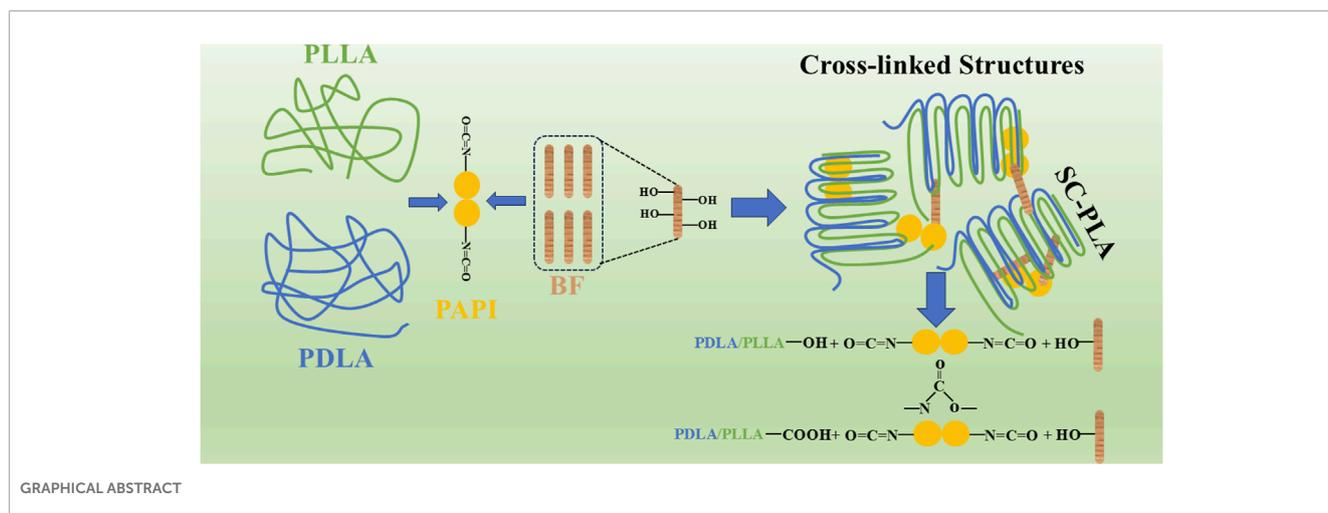
their processing and use (Cheng et al., 2024), people are gradually starting to use biodegradable materials to replace disposable petroleum-based materials (Wan et al., 2024). Poly(lactic acid) (PLA), polyhydroxyalkanoate (PHA), and poly(butylene adipate-co-terephthalate) (PBAT) are common biodegradable plastics (Eraslan et al., 2024). With the continuous progress of technology and good strength comparable to petroleum-based plastics, PLA shows a wider range of applications than other biodegradable plastics (Farkas et al., 2024). However, there are two obvious obstacles to the use and promotion of PLA. The first is its high cost, which is significantly higher than that of petroleum-based materials for the same purpose. Second, the heat resistance of PLA is poor, and its heat resistance temperature is approximately 60°C, which seriously limits its related applications in heat-resistant packaging and food tableware (Zhang et al., 2024).

The main method to reduce the high cost of PLA is to incorporate low-cost fillers, such as biomass and inorganic fillers, into the PLA matrix. The addition of biomass such as starch, wood fiber, and bamboo fiber (BF) to PLA has been widely studied (Khan et al., 2023). Among them, the excellent performance and environmental protection characteristics of BF make it a more suitable biomass filler (Yang et al., 2024). The main ways to improve the heat resistance of PLA include blending heat-resistant materials, increasing crystallinity, and forming stereo-complex (SC) crystals (Nagarajan et al., 2016). There are two types of PLA polymers with different optical activities. When poly-D(lactic acid) (PDLA) and poly-L(lactic acid) (PLLA) are blended, the entanglement between the molecular chains will promote the formation of a stereo-complex crystal form (SC-PLA) (Jia et al., 2024). The melting temperature of the SC-PLA composite is higher than 200°C, which significantly improves the heat resistance of PLA products (Li et al., 2018). However, the cost of PDLA is higher than that of PLLA, and creating the SC-PLA composite increases the cost of PLLA products. This work focuses on whether BF can be used to prepare BF/SC-PLA composites and how to improve the performance of BF/SC-PLA composites. This was because the compatibility between BF and PLA was poor (Chen et al., 2024), and the mechanical properties of BF/SC-PLA composites would be significantly decreased, so

modification methods should be studied to improve the properties of BF/SC-PLA composites.

In recent years, with the continuous attention to the carbon emission and environmental protection characteristics of materials, research on the carbon footprint generated by materials and the related impact on the environment has gradually deepened (Moretti et al., 2021; Schwarz et al., 2023). The life cycle assessment (LCA) analysis is a type of research on the environmental impact and carbon emissions of the whole life cycle of materials (Tamburini et al., 2021; Madival et al., 2009). Even if BF/SC-PLA composites are more environmentally friendly, their manufacturing process will still have some impact on the environment (Beigbeder et al., 2019), and this impact needs to be quantified in this work to ensure the safety and usability of the composites.

In this work, polyaryl polymethylene isocyanate (PAPI) was used to form chemical cross-linked structures with the BF and SC-PLA surface to improve the compatibility of the two phases through the cross-linked structures, and various mechanical properties were tested to explore the best performance of PAPI-modified BF/SC-PLA (PAPI-BF/SC-PLA) composites. In addition, the crystallization properties and heat resistance of different PAPI-BF/SC-PLA composites were investigated. Finally, the LCA analysis was carried out to analyze the PAPI-BF/SC-PLA composite with the best comprehensive performance, and a series of assessments were conducted to study the environmental impact of the composite through substance consumption, CO_2 emissions, and various ecotoxicity effects on the environment. This work provided a reference for the application of API-BF/SC-PLA composites in the fields of heat-resistant packaging and disposable tableware, thus expanding the relevant applications of PLA composites.

2 Materials and methods

2.1 Materials

PLLA (4032D) was purchased from NatureWorks (United States), and PDLA (D70) was purchased from TotalEnergies

TABLE 1 Proportions of different PAPI-BF/SC-PLA.

Name	PLLA (g)	PDLA (g)	BF (g)	PAPI (g)	TMC (g)
TMC + 30%LD	70	30	0	0	0.5
BF-10	63	27	10	0	0.5
BF-15	25.5	59.5	15	0	0.5
BF-20	56	24	20	0	0.5
PAPI-BF-10	63	27	10	5	0.5
PAPI-BF-15	25.5	59.5	15	5	0.5
PAPI-BF-20	56	24	20	5	0.5

Corbion (Thailand). BF was supplied by Jiangxi Zhu Shang Bamboo Industry Co., Ltd. (Jiangxi, China). The sizes of BF were between 100 and 300 meshes. PAPI (44V20) was purchased from Bayer (Germany), with the –NCO groups constituting approximately 30%. TMC-300 was produced by Shaanxi Chemical Research Institute (China). TMC was a suitable nucleating agent for PLA, and its main ingredients were decanedioic acid and 1,10-bis(2-benzoylhydrazine). Acetone was supplied by Sinopharm Group Chemical Reagent Co., Ltd. (China).
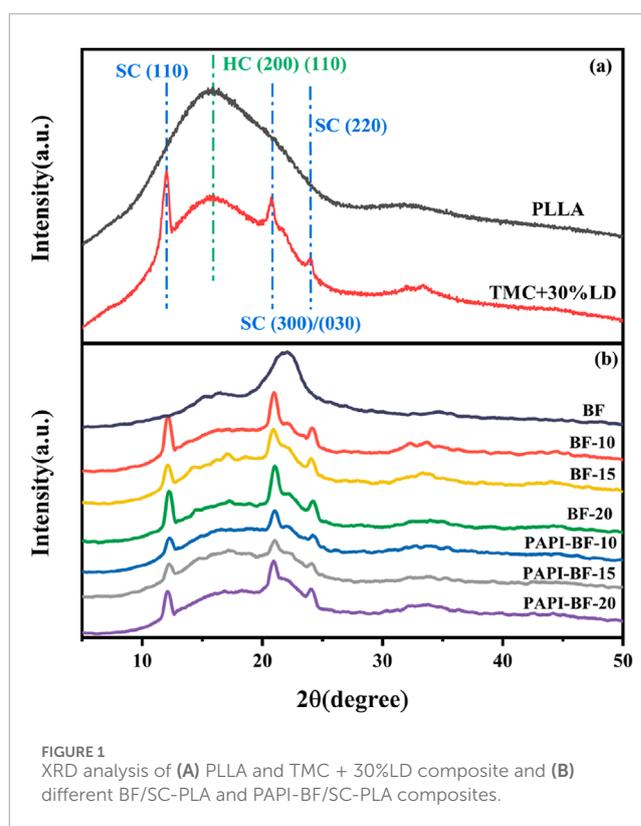
2.2 Sample preparation

PLLA and PDLA pellets were dried at 80°C for 5 h, and BF was dried at 100°C for 5 h. PAPI was weighed according to Table 1, and it was stirred in acetone at two times the volume of PAPI until PAPI was evenly dispersed. The solution was evenly sprayed on the surface of the PLLA/PDLA pellets and then dried at 60°C for 1 h to remove acetone. The sample was named according to the composition of the composite material. Among them, the TMC + 30%LD sample contained 70 wt% PLLA and 30 wt% PDLA. BF-X represented the composites with different BF contents (X represents the added BF content), and PAPI-BF-X represented the composites modified with PAPI. The different pellets were mixed according to the proportions given in Table 1.

The mixed samples were extruded using a twin-screw extruder (SHJ-20, Nanjing Jeante Co., Ltd.), and the processing temperature was 200–220–220–200°C. The composites were injected into splines of various shapes in the injection molding machine (WZS10D, Hongli Machinery Co., Ltd.); the injection temperature was 220°C, and the heating–melting time was 210 s.

FIGURE 1
XRD analysis of **(A)** PLLA and TMC + 30%LD composite and **(B)** different BF/SC-PLA and PAPI-BF/SC-PLA composites.

flexural strength followed the ASTM D790-10 standard (Kartikeyan et al., 2023).

2.3 Mechanical testing of PLA/BF composites

The mechanical strength of the PAPI-BF/SC-PLA composites was assessed using the CMT-5504 Universal Testing Machine (Shenzhen SANS Test Machine Co., Ltd., China). The tensile strength followed the ASTM D638-10 standard, and the

2.4 Characterization of composite properties

The different PAPI-BF/SC-PLA composites were brittle with liquid nitrogen, and the fracture surface was observed using the Quanta 220 scanning electron microscope (FEI Company, United States). The thermodynamics and crystallization properties
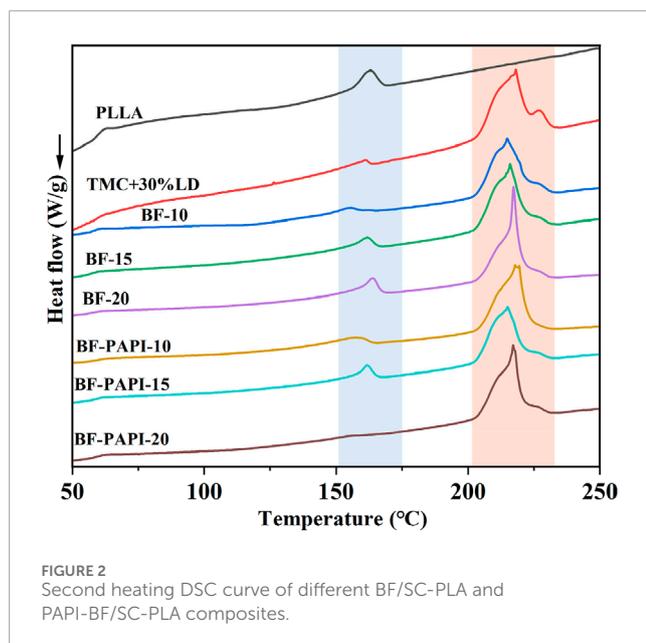
FIGURE 2
Second heating DSC curve of different BF/SC-PLA and PAPI-BF/SC-PLA composites.

of different PAPI-BF/SC-PLA composites were tested using X-ray diffraction (XRD; D/Max-220, Japan) and differential scanning calorimetry (DSC; NETZSCH DSC 214, Germany) analyses referred to in other works (Wan et al., 2024). The contact angle analysis was performed using 4 μL of water using the Biolin Scientific angle measuring instrument (Sweden). The heat-resistant water test of PAPI-BF/SC-PLA composites involved placing the composites in the water under a negative pressure of 10 g heavy weight and then increasing the water temperature to record the shape change of the composites at different water temperatures.

2.5 LCA analysis

The work used LCA Software GaBi Professional, which was developed under the auspices of Argonne National Laboratory. GaBi Professional is the largest and most authoritative LCA database software application based on industrial data. The LCA model is constructed using the ReCiPe2016 v1.1 (H) method (Wernet et al., 2010), which has outstanding comprehensiveness and detail. Based on midpoint and endpoint impact categories, environmental damage types are obtained through classification and characterization to quantify the impact of products on the environment during their whole life cycle. GaBi software was a modular system of plans, processes, and flows with a clear and transparent structure. The data on TMC + 30%LD and its use and electricity were obtained using the software application, and the specific proportion of participating substances is given in Table 1. Regarding power consumption, the TMC + 30%LD composite consumed 0.05 kWh/min according to the processing power of the equipment, and that of the PAPI-BF-20 composite was 0.5 kWh/min. All materials, including BF and PAPI, were calculated as the main raw materials, and their LCA data were obtained from the GaBi Professional database.

3 Results and discussion

3.1 Crystallization property analysis

The XRD analysis was used to analyze the crystallization properties of different BF/SC-PLA and PAPI-BF/SC-PLA composites. The XRD pattern of PLLA showed a wide peak at 16.6°, which belonged to the (200) or (110) crystal plane of homo-crystals (HCs) (Figure 1A) (Wei et al., 2014). Since PLLA was a type of semi-crystalline polymer, its XRD curve showed a wide peak. When PDLA was added to PLLA (TMC + 30%LD composite), two PLA molecular chains with different optical activities were stacked and formed a stereo-complex. This made the TMC + 30%LD composite form SC crystals (Lu et al., 2007). The XRD pattern of the TMC + 30%LD composite showed that the new characteristic peak at 12.1° belonged to the (110) crystal plane, the characteristic peak at 20.7° belonged to the (300)/(030) crystal plane, and the characteristic peak at 23.8° belonged to the (220) crystal plane (Xie et al., 2020). Stereo-complexation occurred between the molecular chains of PLLA and PDLA, and the new SC crystals were formed in the TMC + 30%LD composite. The strong hydrogen bonding between the stereoisomeric molecules significantly improved the heat stability of the TMC + 30%LD composite (Zhang et al., 2021).
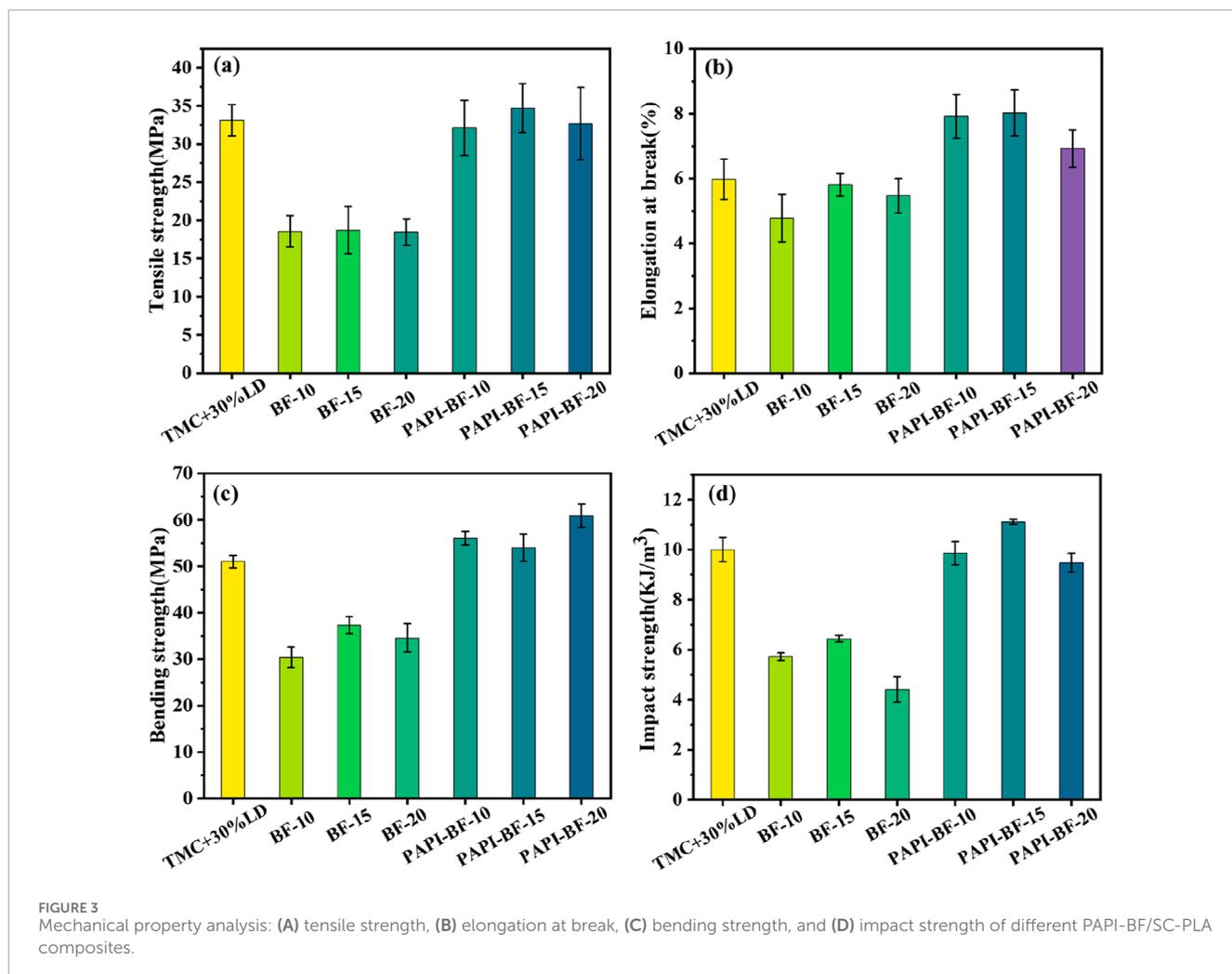
When BF was added, the XRD curves of different BF/SC-PLA composites changed to some extent. The peak strength of HC crystals on the (200) or (110) crystal plane decreased to a certain extent, while the strength of the (300)/(030) crystal plane of SC crystals was significantly increased. This indicated that the heterogeneous nucleation effects of BF were more conducive to the generation of SC crystals and inhibited the generation of HC crystals in PLA composites. The addition of PAPI did not significantly change the crystal shape of different PAPI-BF/SC-PLA composites. In order to prove this phenomenon, the crystallization properties of different BF/SC-PLA composites were further analyzed via DSC analysis.

The second heating DSC curve of different BF/SC-PLA and PAPI-BF/SC-PLA composites is shown in Figure 2. Consistent with XRD results, the strength of HC crystals at approximately 170°C decreased significantly from the PLLA sample to the BF-10 composite when BF was added, which indicated that the heterogeneous nucleation of BF would inhibit the growth of HC crystals and promote the growth of SC crystals in BF/SC-PLA composites.

In addition, DSC analysis showed that the melting temperature of SC crystals of the composite exceeded 220 °C (Malayarom et al., 2023), which indicated that SC crystals could increase the melting temperature, thus improving the heat resistance of the BF/SC-PLA composites. The addition of PAPI had no obvious effect on the crystallization properties of PAPI-BF/SC-PLA composites, which was also consistent with the conclusion obtained from the XRD analysis.

3.2 Mechanical property analysis

The mechanical properties of composites have a very important impact on their applications. The four mechanical properties of

FIGURE 3
Mechanical property analysis: **(A)** tensile strength, **(B)** elongation at break, **(C)** bending strength, and **(D)** impact strength of different PAPI-BF/SC-PLA composites.

different BF/SC-PLA composites after compatible modification using PAPI are shown in Figure 3A. Although stereo-complex crystallites were formed after the addition of PDLA, the tensile strength of the TMC + 30%LD composite was lower than that of most PLLA samples. The multiple crystals in the TMC + 30%LD composite promote the occurrence of crystal phase separations, resulting in its tensile strength decreasing to 33.1 MPa (Chen et al., 2010). Due to the large polarity difference between BF and SC-PLA, the tensile strength of different composites decreased significantly, and that of different composites (BF-10, BF-15, and BF-20 composites) was stable at 18 MPa. When PAPI was used as the interface compatibilizer to modify the BF/SC-PLA composites, isocyanate groups (-NCO) in PAPI could significantly cross-link with hydroxyl groups (-OH) in the molecular chains of PLA and on the surface of BF (Mai et al., 2024). The cross-linked structures formed between the isocyanate and hydroxyl groups could effectively enhance the interaction between BF and SC-PLA and inhibit phase separations (Basil et al., 2023). Thus, the tensile strength of different PAPI-BF/SC-PLA composites was improved. When the content of BF was 15%, the cross-linked effect of PAPI

was most obvious. The tensile strength of the PAPI-BF-15 composite was higher than that of the TMC + 30%LD composite, reaching 34.7 MPa.

PLA was a type of rigid material. The tensile fracture was brittle, and its elongation at break was low, at approximately 6%. With the addition of a more rigid BF, the rigidity of different BF/SC-PLA composites increased further. Regarding the elongation at break (Figure 3B), the cross-linked structures of PAPI could increase the elongation at break of different PAPI-BF/SC-PLA composites. However, due to the strong rigidity of the BF and SC-PLA, the modification effects of PAPI on the elongation at break were very limited, and the highest value of the elongation at break only reached approximately 10% (PAPI-BF-15 composite). The tensile strength of different PAPI-BF/SC-PLA composites was higher than 30 MPa, and the elongation at break was higher than 6%. These strength values were higher than those of other PLA composites used in tableware (Ding et al., 2023).

The modification effect of PAPI on the flexural properties of different BF/SC-PLA composites was most obvious (Figure 3C). BF has a rigid structure, which could act as a skeletal structure in the body to enhance the flexural properties of different
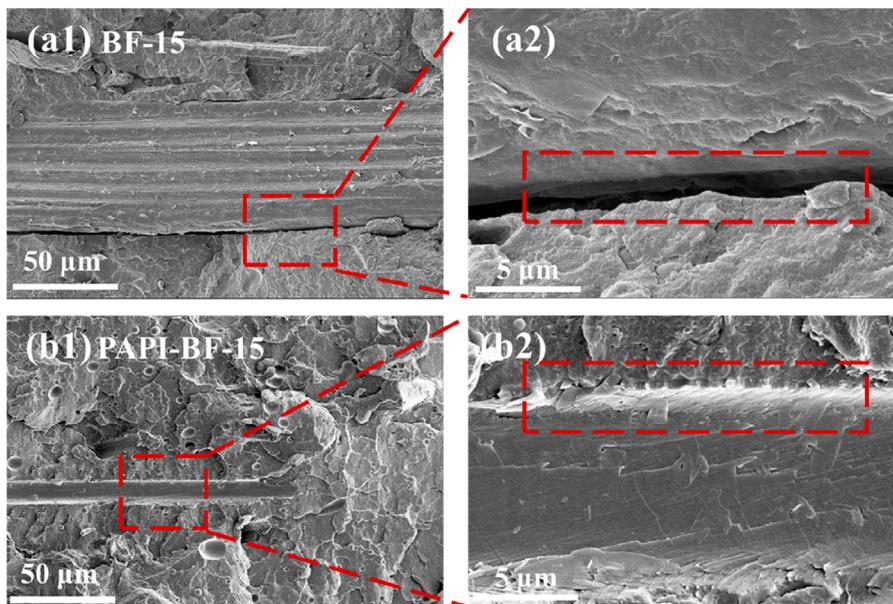
FIGURE 4
The fracture surface of **(a1)** the BF-15 composite, **(a2)** the enlarge of the BF-15 composite, **(b1)** the PAPI-BF-15 composite, and **(b2)** the enlarge of the PAPI-BF-15 composite.
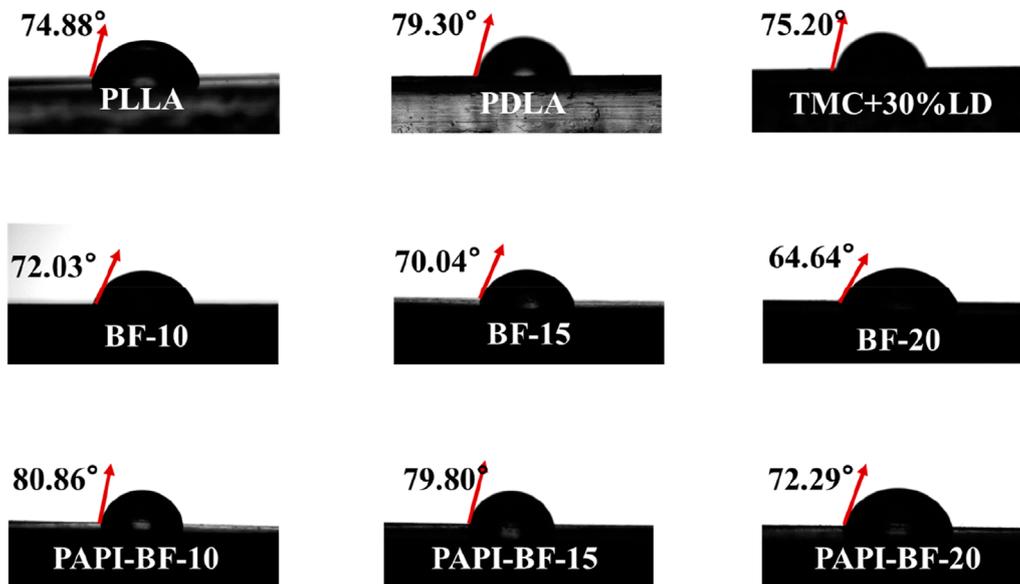

FIGURE 5
Contact angle analysis of different BF/SC-PLA and PAPI-BF/SC-PLA composites.

PLA composites. With the PAPI-cross-linked structure, the compatibility between BF and SC-PLA was improved, and the bending strength of different PAPI-BF/SC-PLA composites was significantly improved. When the content of BF was 20%, the bending strength of the PAPI-BF-20 composite reached 60.9 MPa, which was 19.4% higher than that of the TMC + 30%LD composite, and the bending strength was improved.

The impact strength change trends of different BF/SC-PLA composites were similar to those of tensile strength (Figure 3D). When PAPI promoted the formation of a cross-linked structure between BF and SC-PLA, the impact strength was also improved to a certain extent compared to the TMC + 30%LD composite. All the properties of composites showed that when the content of BF was 15%, the comprehensive properties of the PAPI-BF-20 composite were higher than those of the TMC + 30%LD composite.
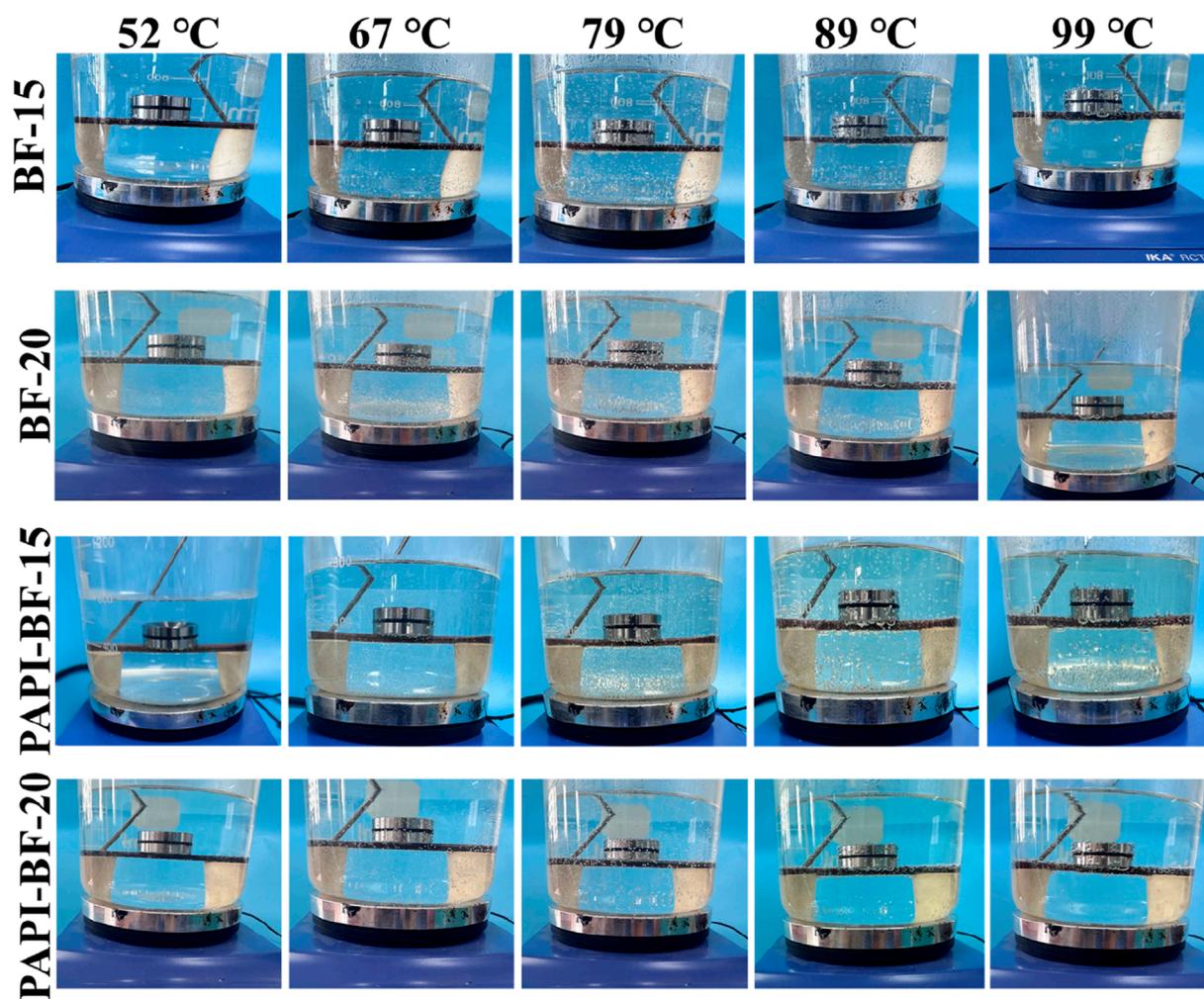
FIGURE 6
Heat-resistance water test of different BF/SC-PLA and PAPI-BF/SC-PLA composites.

3.3 SEM analysis of the fracture surface

The BF-15 and PAPI-BF-15 composites were chosen as examples to show the modification effect of PAPI on the interface between BF and SC-PLA (Figure 4) because the comprehensive mechanical properties of the PAPI-BF-15 composite were the best. The fracture surfaces of the BF-15 and PAPI-BF-15 composites treated with liquid nitrogen were selected to observe SEM images to reveal the reason for the improvement of mechanical performance. In the BF-15 and PAPI-BF-15 composites, BF was wrapped in PLA and dispersed in the PLA matrix (Figures 4a1, 4b1). Due to the polarity difference between BF and SC-PLA, the fracture surface became rough and uneven, and the interface compatibility between BF and SC-PLA also became poor. As shown in Figure 4a2, there was a certain repulsion effect between BF and SC-PLA, which led to an obvious gap between the two terms. Such a gap caused uneven stress transfer during the stress process of the BF-15 composite, resulting in an obvious decrease in the mechanical properties.

After the addition of PAPI, due to the cross-linked structures between isocyanate groups in PAPI and the hydroxyl groups in the

molecular chains of PLA and those on the surface of BF, the cross-linked structures improved the interface compatibility between BF and SC-PLA (Xu et al., 2019). The fracture surface of the PAPI-BF-15 composite became slightly flat, and the gap at the interface of BF and SC-PLA in the PAPI-BF-15 composite disappeared in the SEM image (Figure 4b2). The two phases combined completely and uniformly due to the cross-linked effect of PAPI.

3.4 Contact angle analysis

Contact angle testing of composites could be used to gauge the hydrophobic properties and evaluate the relevant applications in different fields, such as packaging (Figure 5). The contact angle of PLLA was 74.88°, and that of PDLA was 79.30°. The contact angle of the TMC + 30%LD composite was 75.20°, and the contact angle value did not change significantly after the mixing of PLLA and PDLA, indicating that the stereo-complex crystallites of PLA showed no significant effect on the hydrophobicity of PLA composites. The surface of BF contained a large number of hydroxyl groups, so it
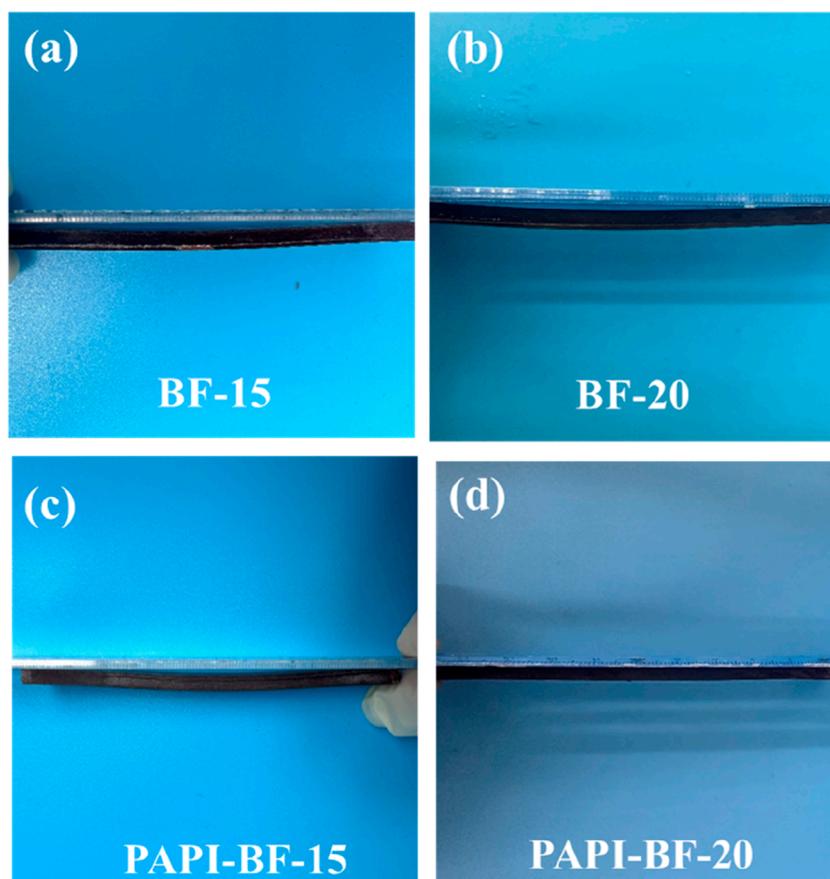
FIGURE 7
Bending diagram of the heat-resistance water properties of **(A)** BF-15, **(B)** BF-20, **(C)** PAPI-BF-15, and **(D)** PAPI-BF-20 composites.

was more hydrophilic. When BF was added to PLA, the contact angle of BF/SC-PLA composites decreased with the increase in BF content, and the lowest angle (BF-20 composite) reached 64.64°. The addition of BF made the different BF/SC-PLA composites more hydrophilic.

However, after the addition of PAPI, due to the reaction between the isocyanate groups and hydroxyl group, a large amount of hydroxyl groups were consumed, which improved the hydrophobicity of the PAPI-BF/SC-PLA composites. When the content of BF was 10%, the contact angle of the PAPI-BF-10 composite was increased to 80.86°. The value of the contact angle was even higher than that of the TMC + 30%LD composite, indicating that the hydrophobicity of the PAPI-BF/SC-PLA composites was enhanced after PAPI was added. This made PAPI-BF/SC-PLA composites more suitable for applications in food packaging and other related fields.

3.5 Heat-resistance water test

As packaging materials or disposable tableware, the materials needed to have a certain heat resistance to ensure that they would not deform at higher temperatures, such as in hot water. The heat resistance of the BF/SC-PLA composites before and

after modification was determined by observing the bending state of the composites at different hydrothermal temperatures. As shown in Figure 6, five different temperature points were used to determine the thermal properties of the BF/SC-PLA composites. The glass conversion temperature of PLA was generally approximately 60°C, so the general use temperature of PLA was slightly higher than 60°C. When PDLA is added, the strong hydrogen bond formed between the SC crystals could effectively improve the heat resistance of the SC-PLA composites.

When BF was added, the heat resistance of the BF/SC-PLA composite was higher than that of pure PLA. Even when the composites were pressed with heavy weights in hot water at 79°C, there was no obvious bending phenomenon. When the water temperature was increased to 89°C, the BF-15, BF-20, and PAPI-BF-15 composites showed a significant bending phenomenon, while the PAPI-BF-20 composite showed no obvious bending phenomenon even at 99°C. When the four composites were removed from the 99-C hot water, obvious bending occurred in the BF-15, BF-20, and PAPI-BF-15 composites, but no obvious deformation occurred in the PAPI-BF-20 composite (Figure 7). This indicated that the cross-linked structures formed after the addition of PAPI and the skeleton structure of BF could effectively inhibit the deformation of the composites in hot water and improve their heat stability. Overall, the PAPI-BF-15 and PAPI-BF-20 composite material is
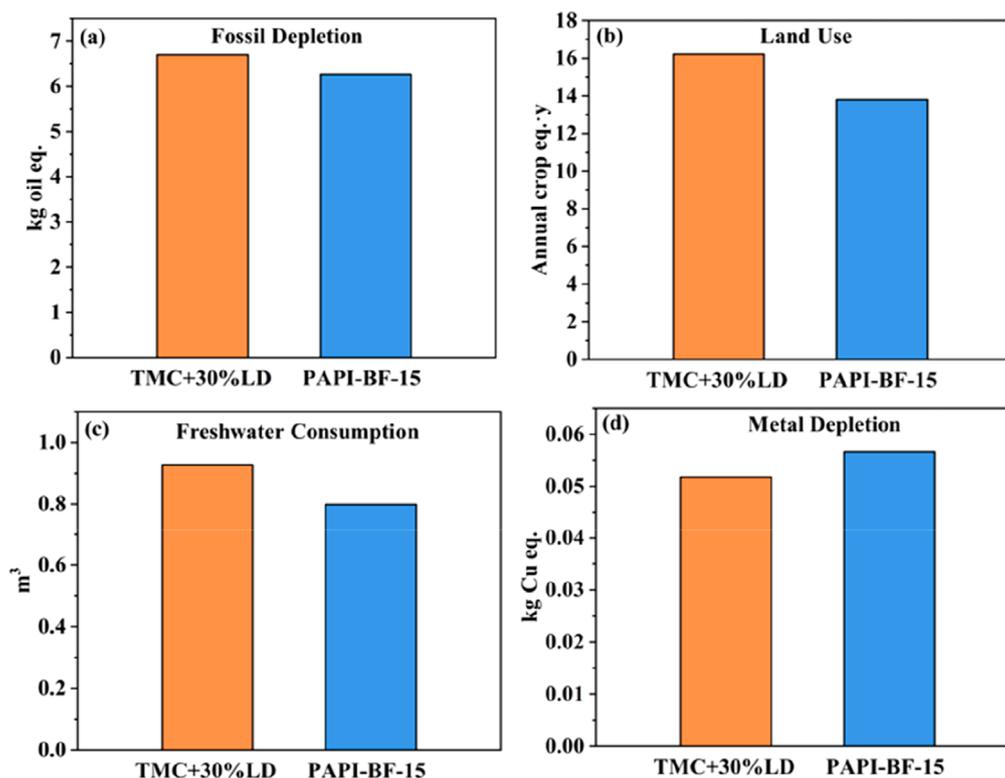
FIGURE 8
Substance consumption: **(A)** fossil depletion, **(B)** land use, **(C)** freshwater consumption, and **(D)** metal depletion of the TMC + 30%LD and PAPI-BF-15 composites.

more suitable for heat-resistant food packaging and disposable tableware compared with the results obtained in other studies (Mai et al., 2024; Ding et al., 2023).

3.6 LCA analysis

The substance consumption of the TMC + 30%LD composite and PAPI-BF-15 composite for the LCA analysis is shown in Figure 8. The PAPI-BF-15 composite was chosen for comparison with the TMC + 30%LD composite in the life cycle assessment was because its various properties were better than those of the TMC + 30%LD composite, which had better possibility in the field of food packaging or disposable tableware.

The carbon source of BF growth mainly came from the CO_2 fixed from the air during its growth, so the BF was a type of negative carbon material. The use of BF showed a positive significance in reducing the utilization of environmental resources (Hermann et al., 2011). When 15% BF was used to prepare the PAPI-BF-15 composite, the composite reduced its fossil depletion by 6.5% compared with the TMC + 30%LD composite. Regarding land use and freshwater consumption (Kolstad et al., 2012), the PAPI-BF-15 composite decreased by 19.9% and 13.8%, respectively, after adding 15% BF. The addition of PAPI in the production of the PAPI-BF-15 composite increased the metal depletion of the composite by 9.5% (Madival et al., 2009). Considering the

abovementioned four main resource consumptions, the PAPI-BF-15 composite had lower resource consumption, as shown by the LCA analysis.

The life cycle assessment of different PLA composites was carried out according to four aspects: (1) carbon emission; (2) PM 2.5 emission; (3) freshwater, marine, and land ecotoxicity; and (4) human toxicity (Figure 9) (Sommerhuber et al., 2017). Due to the addition of BF as a negative carbon material, the whole process of the PAPI-BF-15 composite, from production to use to scrap, had a lower impact than that of the TMC + 30%LD composite in terms of climate change (taking carbon dioxide emission as the standard) and fine particulate-matter formation. The main resource of the CO_2 and particulate matter was the composting and burning of PLA (Rossi et al., 2015). The freshwater, marine, and land ecotoxicity of the PAPI-BF-15 composite were also reduced to a certain extent compared to the TMC + 30%LD composite. Future research could introduce more BF to reduce the corresponding carbon emission of BF/SC-PLA while ensuring the properties of composites.

As a type of biodegradable material, PLA had low toxicity to the human body, and after adding BF, the PAPI-BF-15 composite showed lower toxicity to the human body, which indicated that the PAPI-BF-15 composite could be used in food packaging or disposable tableware and other related fields. In addition, Tran et al. reported that SC-PLA composites could also be composted and degraded (Quynh et al., 2007). Due to the addition of PDLA, the

FIGURE 9
Life cycle assessment of the TMC + 30%LD and PAPI-BF-15 composites regarding four aspects.
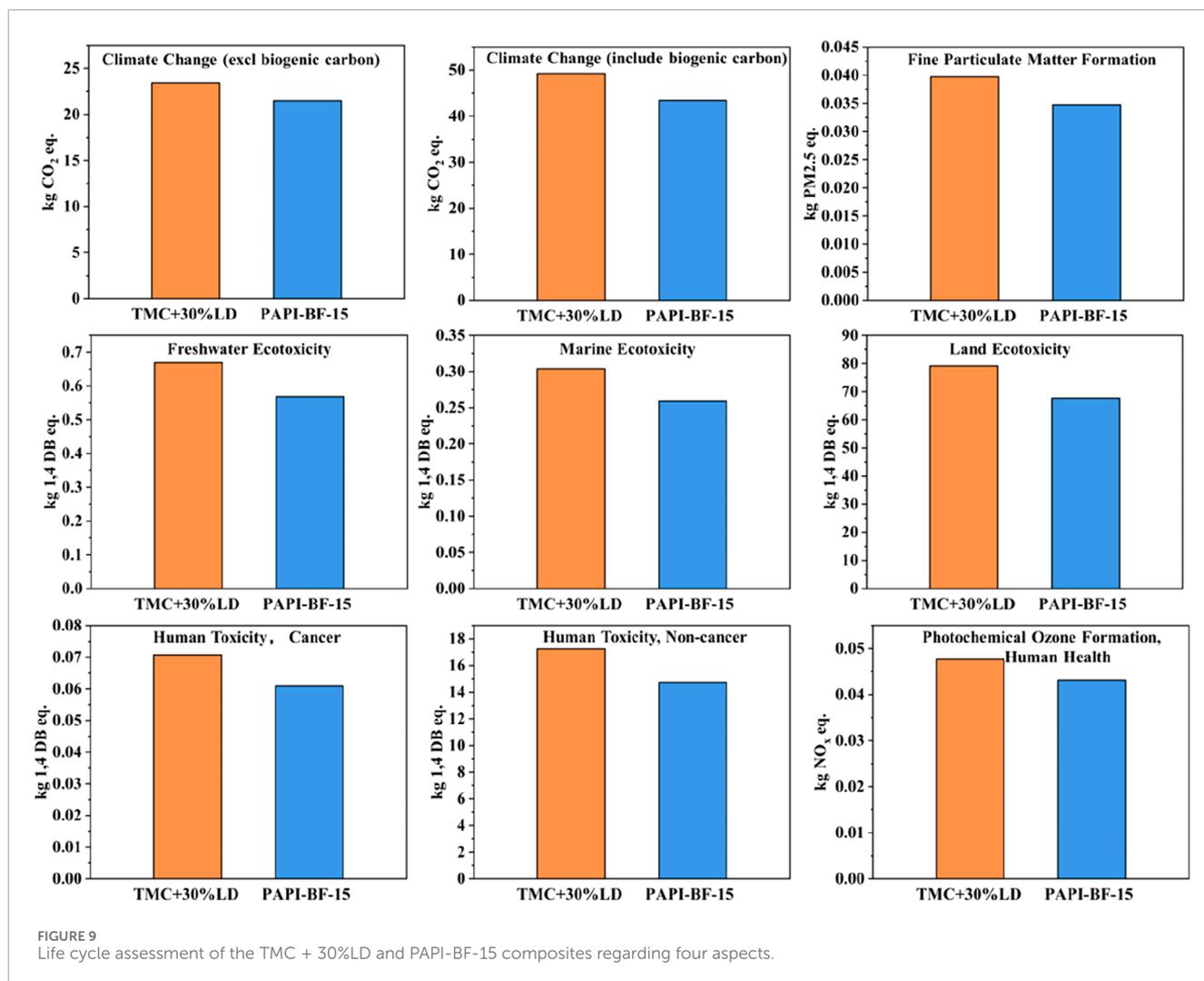
degradation rate of conforming SC-PLA composites would decrease to a certain extent. Various degradation properties of PAPI-BF/SC-PLA composites will also be studied in the following studies to ensure their availability.

4 Conclusion

In this work, the cross-linked effects of PAPI on the crystallization properties, mechanical properties, and heat resistance of PAPI-BF/SC-PLA with different BF contents were studied, and the effects of the modified composites on the environment and carbon emission were evaluated through LCA analysis. The heterogeneous nucleation of BF promoted the formation of SC crystals and inhibited the formation of HC crystals, but the addition of PAPI showed little effect on the crystallization properties. The cross-linked structures formed by PAPI effectively improved the mechanical properties of PAPI-BF/SC-PLA composites. The comprehensive mechanical properties of the PAPI-BF-15 composite were the best because both its tensile strength and flexible strength were higher than those of the TMC + 30%LD composite, and the impact strength increased by 72.6% compared to the PAPI-15 composite and 11.1%

compared to the TMC + 30%LD composite. After the addition of PAPI, the heat resistance of the composites was significantly improved, and the PAPI-BF-20 composite withstood hot water up to 99°C. The LCA analysis showed that the addition of BF effectively reduced the environmental impact and CO_2 emissions of the PAPI-BF-15 composite. The land use and freshwater consumption of the PAPI-BF-15 composite decreased by 19.9% and 13.8%, respectively, after adding 15% BF, while the metal depletion of the composite increased by 9.5%. In addition, the freshwater, marine, and land ecotoxicity of the PAPI-BF-15 composite were also reduced to a certain extent compared to the TMC + 30%LD composite. This study showed that the PAPI-BF-15 composite material was more suitable for heat-resistant food packaging and disposable tableware.

Data availability statement

The original contributions presented in the study are included in the article/Supplementary Material; further inquiries can be directed to the corresponding authors.

Author contributions

Funding

Conflict of interest

The authors declare that the research was conducted in the absence of any commercial or financial relationships that could be construed as a potential conflict of interest.

Publisher's note

All claims expressed in this article are solely those of the authors and do not necessarily represent those of their affiliated organizations, or those of the publisher, the editors, and the reviewers. Any product that may be evaluated in this article, or claim that may be made by its manufacturer, is not guaranteed or endorsed by the publisher.

References

Basil, M., Anirudh, M. K., Lal, A. M. N., Harikrishnan, M., Kundu, P., and Kothakota, A. (2023). Development and characterization of microfiber incorporated with industrial biopolymer composite based biodegradable cutlery: an alternative to single use plastic. *Industrial Crops Prod.* 205, 117526. doi:10.1016/j.indcrop.2023.117526

Beigbeder, J., Soccalingame, L., Perrin, D., Bénézet, J.-C., and Bergeret, A. (2019). How to manage biocomposites wastes end of life? A life cycle assessment approach (LCA) focused on polypropylene (PP)/wood flour and polylactic acid (PLA)/flax fibres biocomposites. *Waste Manag.* 83, 184–193. doi:10.1016/j.wasman.2018.11.012

Chen, B.-K., Shen, C.-H., Chen, S.-C., and Chen, A. F. (2010). Ductile PLA modified with methacryloyloxyalkyl isocyanate improves mechanical properties. *Polymer* 51 (21), 4667–4672. doi:10.1016/j.polymer.2010.08.028

Chen, K., Chen, P., Qi, B., Zhang, X., Cao, L., Sun, C., et al. (2024). Fully bio-based polylactic acid composites based on molecular crosslinking interface engineering. *Compos. Part B Eng.* 283, 111663. doi:10.1016/j.compositesb.2024.111663

Cheng, J., Gao, R., Zhu, Y., and Lin, Q. (2024). Applications of biodegradable materials in food packaging: a review. *Alexandria Eng. J.* 91, 70–83. doi:10.1016/j.aej.2024.01.080

Ding, Y., Ma, H., Liu, X., Qin, S., Liu, J., Qu, G., et al. (2023). Improvement of the mechanical and shape memory properties in polylactide/polyethylene glycol blends by reactive graphene oxide. *Int. J. Biol. Macromol.* 253, 127346. doi:10.1016/j.ijbiomac.2023.127346

Eraslan, K., Altınbay, A., and Nofar, M. (2024). *In-situ* self-reinforcement of amorphous polylactide (PLA) through induced crystallites network and its highly ductile and toughened PLA/poly (butylene adipate-co-terephthalate)(PBAT) blends. *Int. J. Biol. Macromol.* 272, 132936. doi:10.1016/j.ijbiomac.2024.132936

Farkas, C., Gál, L., Csiszár, A., Vincent, G., Jeannin, P.-O., Xavier, P., et al. (2024). Sustainable printed circuit board substrates based on flame-retarded PLA/flax composites to reduce environmental load of electronics: quality, reliability, degradation and application tests. *Sustain. Mater. Technol.* 40, e00902. doi:10.1016/j.susmat.2024.e00902

Hermann, B. G., Debeer, L., De Wilde, B., Blok, K., and Kumar Patel, M. (2011). To compost or not to compost: carbon and energy footprints of biodegradable materials' waste treatment. *Polym. Degrad. Stab.* 96 (6), 1159–1171. doi:10.1016/j.polymdegradstab.2010.12.026

Jia, H., Hou, Y., Zhang, M., Pan, Y., Liu, C., Shen, C., et al. (2024). SC crystals of porous PLA via thermally–induced phase separation: effects of process conditions, solvent composition and nucleating agent. *Eur. Polym. J.* 213, 113095. doi:10.1016/j.eurpolymj.2024.113095

Kartikeyan, B., Ponshanmugakumar, A., Saravanan, G., BharathGanesh, S., and Hemamalini, V. (2023). "Experimental and theoretical analysis of FDM AM PLA mechanical properties," in *Materials today: proceedings*.

Khan, A., Sapuan, S. M., Yusuf, J., Uddin Siddiqui, V., Zainudin, E. S., Zuhri, M. Y. M., et al. (2023). An examination of cutting-edge developments in Bamboo-PLA composite research: a comprehensive review. *Renew. Sustain. Energy Rev.* 188, 113832. doi:10.1016/j.rser.2023.113832

Kolstad, J. J., Vink, E. T. H., De Wilde, B., and Debeer, L. (2012). Assessment of anaerobic degradation of Ingeo™ polylactides under accelerated landfill conditions. *Polym. Degrad. Stab.* 97 (7), 1131–1141. doi:10.1016/j.polymdegradstab.2012.04.003

Li, Y., Qiao, L., Yang, G., Ming, R., Yu, M., Zhang, H., et al. (2018). Evaluation of thermal resistance and mechanical properties of injected molded stereo-complex of poly (l-lactic acid) and poly (d-lactic acid) with various molecular weights. *Adv. Polym. Technol.* 37 (6), 1674–1681. doi:10.1002/adv.21824

Lu, J., Huang, R., and Oh, I.-K. (2007). Morphology investigation on high-pressure crystallized bisphenol-A polycarbonate/dioctyl phthalate blends. *J. Polym. Sci. Part B Polym. Phys.* 45 (19), 2715–2728. doi:10.1002/polb.21192

Madival, S., Auras, R., Singh, S. P., and Narayan, R. (2009). Assessment of the environmental profile of PLA, PET and PS clamshell containers using LCA methodology. *J. Clean. Prod.* 17 (13), 1183–1194. doi:10.1016/j.jclepro.2009.03.015

Mai, V.-D., Kang, D., Kim, Y., Jang, Y., Min, J., Han, J., et al. (2024). Preparation and environmental analysis of biodegradable polylactic acid and modified cellulose nanofiber composites. *J. Industrial Eng. Chem.* 130, 401–411. doi:10.1016/j.jiec.2023.09.046

Malayarom, P., Pongpakdee, C., and Pattamaprom, C. (2023). Fine-tuning heat resistance and impact toughness of natural rubber-toughened PLA at Various degrees of PLA/PDLA stereocomplexation. *Compos. Part C. Open Access* 12, 100391. doi:10.1016/j.jcomc.2023.100391

Moretti, C., Hamelin, L., Jakobsen, L. G., Junginger, M. H., Steingrimsdottir, M. M., Høibye, L., et al. (2021). Cradle-to-grave life cycle assessment of single-use cups made from PLA, PP and PET. *Resour. Conservation Recycl.* 169, 105508. doi:10.1016/j.resconrec.2021.105508

Nagarajan, V., Mohanty, A. K., and Misra, M. (2016). Perspective on polylactic acid (PLA) based sustainable materials for durable applications: focus on toughness and heat resistance. *ACS Sustain. Chem. and Eng.* 4 (6), 2899–2916. doi:10.1021/acssuschemeng.6b00321

Quynh, T. M., Mitomo, H., Nagasawa, N., Wada, Y., Yoshii, F., and Tamada, M. (2007). Properties of crosslinked polylactides (PLLA and PDLA) by radiation and its biodegradability. *Eur. Polym. J.* 43 (5), 1779–1785. doi:10.1016/j.eurpolymj.2007.03.007

Rossi, V., Cleeve-Edwards, N., Lundquist, L., Schenker, U., Dubois, C., Humbert, S., et al. (2015). Life cycle assessment of end-of-life options for two biodegradable packaging materials: sound application of the European waste hierarchy. *J. Clean. Prod.* 86, 132–145. doi:10.1016/j.jclepro.2014.08.049

Schwarz, A., Ferjan, Š., and Kunst, J. (2023). Life cycle assessment of advanced grade PLA product with novel end-of-life treatment through depolymerization. *Sci. Total Environ.* 905, 167020. doi:10.1016/j.scitotenv.2023.167020

Sommerhuber, P. F., Wenker, J. L., Rüter, S., and Krause, A. (2017). Life cycle assessment of wood-plastic composites: analysing alternative materials and identifying an environmental sound end-of-life option. *Resour. Conservation Recycl.* 117, 235–248. doi:10.1016/j.resconrec.2016.10.012

Tamburini, E., Costa, S., Summa, D., Battistella, L., Fano, E. A., and Castaldelli, G. (2021). Plastic (PET) vs bioplastic (PLA) or refillable aluminium bottles–What is the most sustainable choice for drinking water? A life-cycle (LCA) analysis. *Environ. Res.* 196, 110974. doi:10.1016/j.envres.2021.110974

Wan, H., Sun, C., Xu, C., Wang, B., Chen, Y., Yang, Y., et al. (2024). Synergistic reinforcement of polylactic acid/wood fiber composites by cellulase and reactive extrusion. *J. Clean. Prod.* 434, 140207. doi:10.1016/j.jclepro.2023.140207

Wei, X. F., Bao, R. Y., Cao, Z. Q., Yang, W., Xie, B. H., and Yang, M. B. (2014). Stereocomplex crystallite network in asymmetric PLLA/PDLA blends: formation, structure, and confining effect on the crystallization rate of homocrystallites. *Macromolecules* 47, 1439–1448. doi:10.1021/ma402653a

Wernet, G., Conradt, S., Isenring, H. P., Jiménez-González, C., and Hungerbühler, K. (2010). Life cycle assessment of fine chemical production: a case study of pharmaceutical synthesis. *Int. J. Life Cycle Assess.* 15, 294–303. doi:10.1007/s11367-010-0151-z

Xie, Q., Guo, G., Lu, W., Sun, C., Zhou, J., Zheng, Y., et al. (2020). Polymorphic homocrystallization and phase behavior of high-molecular-weight Poly (L-lactic acid)/poly (D-lactic acid) racemic mixture with intentionally enhanced stereocomplexation ability via miscible blending. *Polymer* 201, 122597. doi:10.1016/j.polymer.2020.122597

Xu, F. L., Hu, R. R., and Park, S. J. (2019). Improvement of thermal behaviors of biodegradable poly (lactic acid) polymer: a review. *Compos. Part B Eng.* 164, 287–296. doi:10.1016/j.compositesb.2018.10.078

Yang, Y., Han, W., Wang, B., Wang, B., Chen, K., Tan, H., et al. (2024). Preparation and properties of bamboo fiber/polylactic acid composite modified with polycarbodiimide. *Industrial Crops Prod.* 218, 118829. doi:10.1016/j.indcrop.2024.118829

Zhang, J., Peng, L., Li, Y., Luo, M., Yan, Z., Wang, T., et al. (2024). Preparation of PLA/PBAT blends with high performance via the synergistic effect of high mold temperature and strong shear field. *Polymer* 296, 126795. doi:10.1016/j.polymer.2024.126795

Zhang, X. X., Yang, S.-G., Zhong, G.-J., Lei, J., Liu, D., Sun, G.-A., et al. (2021). Rapid melt crystallization of bisphenol-A polycarbonate jointly induced by pressure and flow. *Macromolecules* 54 (5), 2383–2393. doi:10.1021/acs.macromol.0c02208

Nomenclature

PLA	Poly(lactic acid)
LCA	Life cycle assessment
PAPI	Polyaryl polymethylene isocyanate
BF	Bamboo fiber
SC-PLA	Stereo-complex crystal PLA
BF/SC-PLA	Bamboo fiber/stereo-complex crystal PLA composites
PAPI-BF/SC-PLA	PAPI-modified bamboo fiber/stereo-complex crystal PLA composites
PHA	Polyhydroxyalkanoate
PBAT	Poly(butylene adipate-*co*-terephthalate)